Lab on a Chip

Cite this: *Lab Chip*, 2012, **12**, 640

www.rsc.org/loc

PAPER

Microfluidic wound-healing assay to assess the regenerative effect of HGF on wounded alveolar epithelium†

Marcel Felder,‡[a] Pauline Sallin,‡[ab] Laurent Barbe,[b] Beat Haenni,[c] Amiq Gazdhar,[de] Thomas Geiser[de] and Olivier Guenat*[ab]

Received 13th September 2011, Accepted 15th November 2011
DOI: 10.1039/c1lc20879a

We present a microfluidic epithelial wound-healing assay that allows characterization of the effect of hepatocyte growth factor (HGF) on the regeneration of alveolar epithelium using a flow-focusing technique to create a regular wound in the epithelial monolayer. The phenotype of the epithelial cell was characterized using immunostaining for tight junction (TJ) proteins and transmission electron micrographs (TEMs) of cells cultured in the microfluidic system, a technique that is reported here for the first time. We demonstrate that alveolar epithelial cells cultured in a microfluidic environment preserve their phenotype before and after wounding. In addition, we report a wound-healing benefit induced by addition of HGF to the cell culture medium (19.2 *vs.* 13.5 μm h^{-1} healing rate).

1. Introduction

Pulmonary fibrosis is a chronic disease of a variety of different etiologies that is characterized by the formation of excessive connective tissue (fibrosis) in the lungs. It causes progressive scarring of interstitial tissues and restricts the patients of their ability to breathe. Idiopathic pulmonary fibrosis (IPF) is one of the deadliest and most common forms of pulmonary fibrosis;[1] the etiology and exact pathophysiology are still unknown. Recent evidence led to the hypothesis suggesting improper alveolar reepithelization in response to microinjuries as a trigger for fibrotic processes.[2] The sequential microinjuries lead to disruption of alveolar epithelial integrity.

The restoration of an intact epithelium following injury is therefore a crucial phase of normal wound-healing. Unfortunately, no proven effective therapies are available to date for the treatment of pulmonary fibrosis beyond lung transplantation.[3] Recent research emphasis has been placed on targeting the molecular events that are believed to perpetuate and sustain the fibrotic process in IPF and restore the injured alveolar epithelium.[4] Some anti-fibrotic therapies are emerging based on either the inhibition of profibrotic mediators, *e.g.* TGF-beta,[4] or the overexpression of epithelial growth factors, which have anti-fibrotic and regenerative properties. Among those, hepatocyte growth factor (HGF) is known to increase epithelial cells motility, survival and proliferation and thus alveolar reepithelization.[5–8]

However, the critical mechanisms of HGF induced fibrotic remodelling and regeneration still remains poorly understood.[5] To tackle this challenge, new tools and methods are clearly needed to evaluate and examine epithelial repair mechanisms *in vitro* and *in vivo*.[6] Recently, a microfabricated soft elastic microstencil[9] consisting of an array of long rectangular trenches in which kidney epithelial cells were grown to confluence was employed to replace the traditional scratch tests used in standard wound-healing assays.[10,11] In sharp contrast to scratch tests performed with a sterile glass or a plastic pipette tip, which detaches and damages the cells, leading to the release of intracellular content and cellular debris into the nutrition medium, the latter technique did not traumatize the cells located at the edge of the wound. This study showed that *in vitro* wound-healing processes are not necessarily dependent on cell injury and can even be induced in the absence of cell damage.

Microfluidic devices that allow to better mimic the *in vivo* physiological conditions *in vitro*[12] may play a leading role in studying the epithelial repair mechanism, in particular because the cellular microenvironment can be better controlled than in standard *in vitro* cell cultures. In such systems, the cell milieu is well regulated and can be controlled in a very precise manner, and the readouts are more accurate. In the present study, we analyse the effects of HGF on alveolar epithelial regeneration in a microfluidic model. In this system, lung epithelial cells are confined in a small microchannel leading to a reduction of the

[a]*University of Berne, ARTORG Lung Regeneration Technologies Lab, Murtenstrasse 50, CH-3010 Berne, Switzerland. E-mail: olivier.guenat@artorg.unibe.ch; Fax: +41 31 632 7576; Tel: +41 31 632 7608*
[b]*CSEM SA, Nanomedicine Division, Bahnhofstrasse 1, CH-7302 Landquart, Switzerland*
[c]*University of Berne, Institute of Anatomy, Baltzerstrasse 2, CH-3012 Berne, Switzerland*
[d]*University Hospital of Berne, Division of Pulmonary Medicine, Freiburgstrasse 3, CH-3010 Berne, Switzerland*
[e]*University of Berne, Department of Clinical Research, Murtenstrasse 50, CH-3010 Berne, Switzerland*
† Electronic supplementary information (ESI) available: See DOI: 10.1039/c1lc20879a
‡ Authors contributed equally.

dilution of secreted cell signalling molecules and may adequately be used in applications for which controlled and regulated environments are required. The alveolar epithelium was wounded in the microchannel by a laminar flow of trypsin focused between two adjacent flows of the cell culture medium.[13] A similar flow focusing technique was recently used in migration assays for fibroblasts[14] and endothelial cells.[15] The effect of HGF on epithelial regeneration is characterized and discriminated from the effect upon serum exposure. Furthermore, the specific characteristics of alveolar epithelial cells are investigated before wounding and after epithelial regeneration using immunostaining for cell junction proteins and transmission electron micrographs (TEMs). It is the first time that this technique is reported for cells grown in a microchannel to the best of our knowledge.

2. Materials and methods

2.1. Device design and fabrication

The microfluidic platform is composed of a microchannel serving as a cell culture microwell. This 900 μm wide, 100 μm high and 14 mm long microchannel has a volume of 1.26 μl, and is connected on each side by two inlets and three outlets (Fig. 1). The cross-section of the inlet and outlet microchannels is 260 μm wide by 100 μm high. Inlet microchannels 1 and 2 are 12 mm long, whereas the outlet microchannels are each 6 mm long. The devices are fabricated with poly(dimethylsiloxane) (PDMS, Dow Corning) using soft lithography techniques[16] from masters prepared by photolithography using an SU-8 photoresist (Microchem, USA) on 100 mm diameter silicon wafers. Each chip is plasma-bonded to glass and contains two identical platforms as illustrated in Fig. 1.

2.2. Cell culture and cell seeding in the microfluidic platform

All cell manipulations were performed in a sterile flow hood and incubation was done in a standard 5% CO_2 cell incubator at 37 °C. The human alveolar epithelial-like cell line A549 (passages 25–40) was obtained from ATCC. A549 cells were maintained in RPMI 1640 medium (Gibco) supplemented with 100 U ml^{-1} penicillin, 100 μg ml^{-1} streptomycin (penicillin–streptomycin, Invitrogen) and 10% of fetal bovine serum (FBS, Gibco). The latter solution will be identified by the term "enriched RPMI" in the following. Passages were done twice a week using 0.25% trypsin with EDTA·4Na (Gibco). Cell counting was performed after Trypan blue staining (Trypan blue stain 0.4%, Invitrogen) by an automated cell counter (Countness™, Invitrogen). On reaching approximately 90% confluence, the A549 cells were washed twice with phosphate-buffered saline (PBS, Gibco), removed from the flask by the addition of 0.25% trypsin and washed with enriched RPMI. The cells were concentrated by centrifugation to reach a concentration of 6×10^6 cells ml^{-1} after resuspension in enriched RPMI.

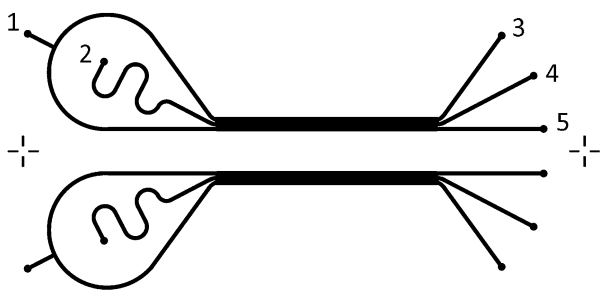

Fig. 1 Schematic view of the microfluidic platform with two independent microchannels. Inlet 2 and outlet 4 are used for the cell seeding and perfusion, whereas inlet 1, outlet 3 and outlet 5 are exclusively used for the trypsin wounding and plugged for all other experiments.

Prior to cell seeding, the microchannels were rinsed with isopropanol followed by deionised water. Then, enriched RPMI was inserted into the microchannels for 2 hours at 37 °C to allow protein adsorption onto the microchannel walls. Cell seeding was performed by delivering a 20 μl droplet of a concentrated cell suspension (6×10^6 cells ml^{-1}) at inlet 2, and temporarily tilted in order to create a small hydrostatic pressure difference between inlet 2 and outlet 4 (Fig. 1), generating a small flow rate in the microchannel allowing cell inoculation. After this procedure, cells were allowed to attach to the glass substrate for 3 hours. Then, inlet 2 of the microchannel was connected to a horizontally oriented 1 ml syringe reservoir (see ESI, Fig. S1†) for medium perfusion. The diameter of these syringe (1 ml syringe, U-100 Insulin, VWR) reservoirs was small enough to prevent the solution from leaking.[17] Outlet 4 of the microchannel was connected to a peristaltic pump (ISM834C, Ismatec, Switzerland) to pull the solution off the syringe reservoirs, whereas inlet 1 and the lateral outlets 3 and 5 were sealed using pipette-tip plugs. For all experiments the cell cultures were perfused for one minute at 3.4 μl min^{-1} every 30 minutes. Cell confluency was reached after two days.

For closer examination of the wound-healing processes, we treated the confluent layer of A549 cells with mitomycin C (10 μg ml^{-1}) in serum-free medium for 2.5 hours at 37 °C. Mitomycin C is an anti-neoplastic antibiotic that intercalates with the DNA of cells and inhibits the DNA synthesis, thus it blocks cellular proliferation.

2.3. Wound creation and healing protocols

A wound-healing model was used to mimic epithelial injury and to study the regeneration and repair of the alveolar epithelium. Once confluent, the A549 epithelial layer was washed with PBS and was then wounded by using a flow focusing technique, enabling the creation of a confined flow of trypsin in the central part of the microchannel, surrounded by lateral flows of enriched RPMI. The focused flow was created by drawing a 10-fold concentrated trypsin (2.5%) and enriched RPMI contained in pipette-tip inlet reservoirs with a peristaltic pump located downstream. Trypsin is a proteolytic enzyme that is routinely used to dissociate adherent cells *via* cleavage of extracellular proteins. The enzymatic activity is optimal at a physiologic temperature of 37 °C, therefore the wounding assay was performed on a hotplate. Consequently, cells located in the central part of the microchannel were detached gently, while the cells adjacent to the trypsin flow were exposed to enriched RPMI and remained unaffected. The cells were wounded at a constant flow rate of 3.4 μl min^{-1} during 5 to 7 minutes (Fig. 2). After wounding, the microchannel was washed and perfused for an additional two minutes with enriched RPMI. The whole wound creation procedure was performed on a hotplate at 37 °C.

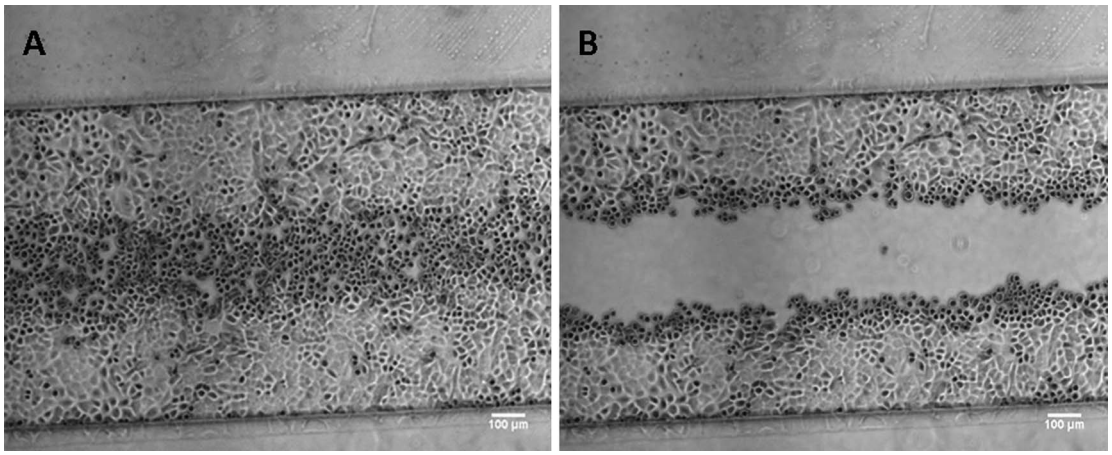

Fig. 2 Microscopic phase contrast pictures of an epithelial A549 cell layer in a microchannel, after 4 (A) and 7 min (B) of exposure to a focused flow of trypsin.

After wounding, serum-free or enriched RPMI ± 10 ng ml^{-1} HGF (294-HG-005, R&D Systems, Switzerland) was used to perfuse the cell culture at an intermittent flow rate of 3.4 µl min^{-1} for one minute every 30 minutes. The wound closure rate was monitored with an inverted microscope (VWR IT400, 3.4×) equipped with a digital camera (Moticam 1000, VWR). Pictures were taken at fixed positions in the epithelial wound at different time intervals (0, 2, 5, 9 and 13 hours post-injury). Subsequently, the wound area in each picture was determined by outlining and quantifying the wound width and area using ImageJ image processing software.[18] Linear regression analysis of the wound width in a representative image sequence was used to determine the wound-healing rate in µm h^{-1}. The wound closure degree was calculated as a percentage of the difference between the initial wound area and the remaining wound area divided by the initial wound area.[19] The data are shown as means with 95% CI (Confidence Interval). Three conditions were investigated: serum-free, enriched and HGF-supplemented enriched media. For each condition, assays were performed in four microchannels, within which the wound area and the wound width were measured at five different locations.

2.4. Immunostaining and fluorescence imaging

A549 cells were cultured on the microfluidic platform and grown to confluence. For immunohistochemical characterization, the cells were washed three times with PBS and fixed with 3% paraformaldehyde in PBS for 15 min at room temperature. Prior to the incubation of primary and secondary antibodies, the PDMS cover was gently removed from the glass slide, by sliding a scalpel tip between the glass and the PDMS, in order to avoid the loss of signal intensity through the PDMS. Fixed cells were treated with 0.1 M glycine (VWR) in PBS for 5 min and permeabilized in 0.2% Triton X-100 (AppliChem, Switzerland) in PBS for 15 min as described by Blank *et al.*[20] Primary antibodies for ZO-3 (rabbit anti-human, 1 : 100, Zymed) were diluted in bovine serum albumin (BSA, Sigma) 1 mg ml^{-1} PBS and incubated for 60 min in a moist chamber at room temperature. Cells were washed three times with PBS and incubated with secondary antibody (goat anti-rabbit IgG, 1 : 100, Abcam, USA), followed by nuclear counterstaining and mounting in DAPI Vectashield Mounting Media (Vector Laboratories).

2.5. Sample preparation for TEM analysis

For TEM investigations, pre-wounded and regenerated samples were fixed with 2.5% glutaraldehyde (Agar Scientific Ltd., Cambridge) in 0.15 M Hepes (Sodium salt, Fluka) buffer at 4 °C for at least 24 h. Samples were further postfixed in 0.1 M Na-cacodylate (Merck) buffered 1% OsO_4 (SPI Supplies, West Chester, USA) for 1 h and contrasted with 0.5 M maleate–NaOH (Merck) buffered 0.5% uranylacetate (Fluka). After dehydration in graded series of ethanol, the microfluidic channels were filled with Epon (Fluka) by capillary forces (Fig. 3). Epon was polymerized at 60 °C for 4 to 5 days. Then, the microfluidic platforms containing the Epon-embedded A549 cells were repeatedly dipped into liquid nitrogen, inducing a mechanical stress due to the different thermal expansion coefficients[21] between glass and PDMS, until separation of the PDMS from the glass slide. The preparations were embedded a second time to enable horizontal and vertical sectioning in 70–80 nm ultrathin slices.

Finally, the slices are transferred on Formvar-coated one-hole grids, double stained with lead citrate and uranylacetate and investigated using a Philips CM 12 transmission electron microscope (FEI Co. Philips Electron Optics, Zurich, Switzerland).

3. Results and discussion

The volume of the microchannel (without inlets and outlets) being 1.26 µl, the cell culture supernatant was completely renewed each half an hour. At this flow rate, the Reynolds number of the microfluidic platform was 0.12, indicating that the laminar flow was stably formed in the whole microchannel, and that two or more streams flowing in contact with each other did not mix except by diffusion at the interface.

The lung epithelial cell cultures in the microfluidic platform were characterized in four general steps. First, alveolar epithelial cells were cultured, grown to confluence in the microfluidic platform and characterized to demonstrate that the phenotype of

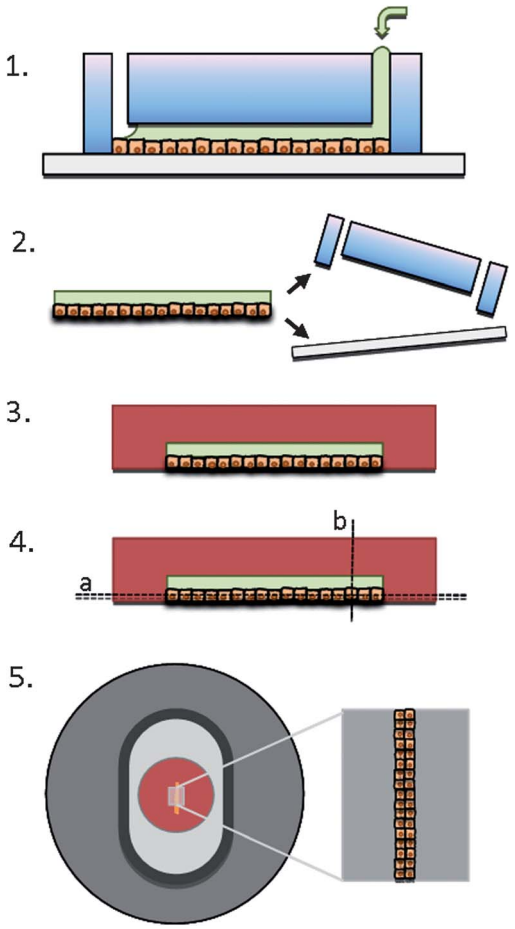

Fig. 3 Schematic representation of TEM sample preparation. (1) Epon is introduced into the microchannel on fixed cells by capillary forces. (2) PDMS and the glass slide are removed by the mechanical stress created by liquid nitrogen in which they are dipped repeatedly. (3) A second Epon layer further embeds the sample; it is followed by (4) horizontal and vertical sectioning using an ultramicrotome. (5) Ultrathin sections are transferred to Formvar-coated one-hole grids for TEM observations.

A549 cells could be maintained in the microchannel. Second, a wound was created in the confluent epithelial layer, using a focused flow of trypsin, allowing the selective removal of the cells in the central part of the microchannel. The aim of the third phase was to study the regeneration of the wounded epithelial layer exposed to HGF. Finally, the regenerated epithelium was investigated in terms of preservation of the phenotype, in particular the generation of lamellar bodies and extensive cellular junctions that are typical features of an intact type II alveolar epithelial layer.

3.1. Characterization of the A549 alveolar epithelial cell layer cultured in the microfluidic platform

The A549 epithelial cell cultures were characterized according to their typical features (*i.e.* morphology of the cells, integrity of the epithelial layer and expression of specific cell surface markers).

Two days after cell seeding, the epithelial cells reached confluence in the microfluidic platform and homogeneously covered the entire microchannel (Fig. 4a). Confluent alveolar epithelial cells typically grow in tight monolayers with extensive cell–cell contacts. These contacts result from membrane protein connections in the intercellular space that forms an impermeable barrier to fluid. They are composed of transmembrane proteins (*e.g.* occludins and claudins) and associated cytoplasmic proteins (*e.g.* zonula occludens and cingulin) that link the tight junction plaques to the actin cytoskeleton. The expressions of these tight junction proteins were investigated by immunostaining. Occludin and zonula occludens-3 (ZO-3) expressions are illustrated in Fig. 4b and c, respectively. Accumulation of occludin and ZO-3 at the cellular interfaces can clearly be observed, confirming the formation of strong cell–cell contacts. The expressions are weaker in some parts of the microchannel, but it is well known that A549 cell monolayers weakly express occludin and ZO-3.[20,22] We observed that the expression of tight junction proteins is a highly dynamic process and that the *in vitro* assembly is highly linked to the confluence state of the epithelial layer. Before confluence and at the over-confluent state (cells starting to form a second layer), occludin and ZO-3 staining appeared mainly as punctated aggregates in the perinuclear zone and was just occasionally located at the cell–cell interfaces. It was therefore found critical to perform immunostaining at confluence.

TEM was used to characterize the integrity of the epithelial cell layer, as well as to identify typical ultrastructures of type II alveolar epithelial cells. After fixation, the cells were embedded in Epon that was introduced into the microchannel by capillary forces. Following polymerization, the preparations were cut either horizontally (Fig. 5) or vertically (Fig. 8). At higher magnification, the lamellar bodies, which store and secrete pulmonary surfactant and are typical hallmarks of type II alveolar epithelial cells, can clearly be recognized (Fig. 5c). In Fig. 5d,

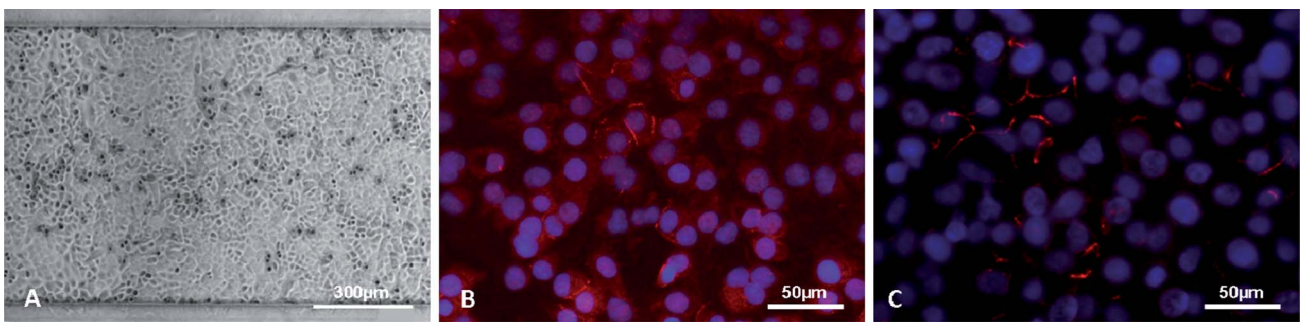

Fig. 4 Microscopic images of confluent A549 cells after two days of culturing in the microfluidic platform, before being wounded. (A) Phase contrast picture, and fluorescent images of (B) occludin and (C) Z0-3 expressions, with the cell nuclei counterstained with DAPI.

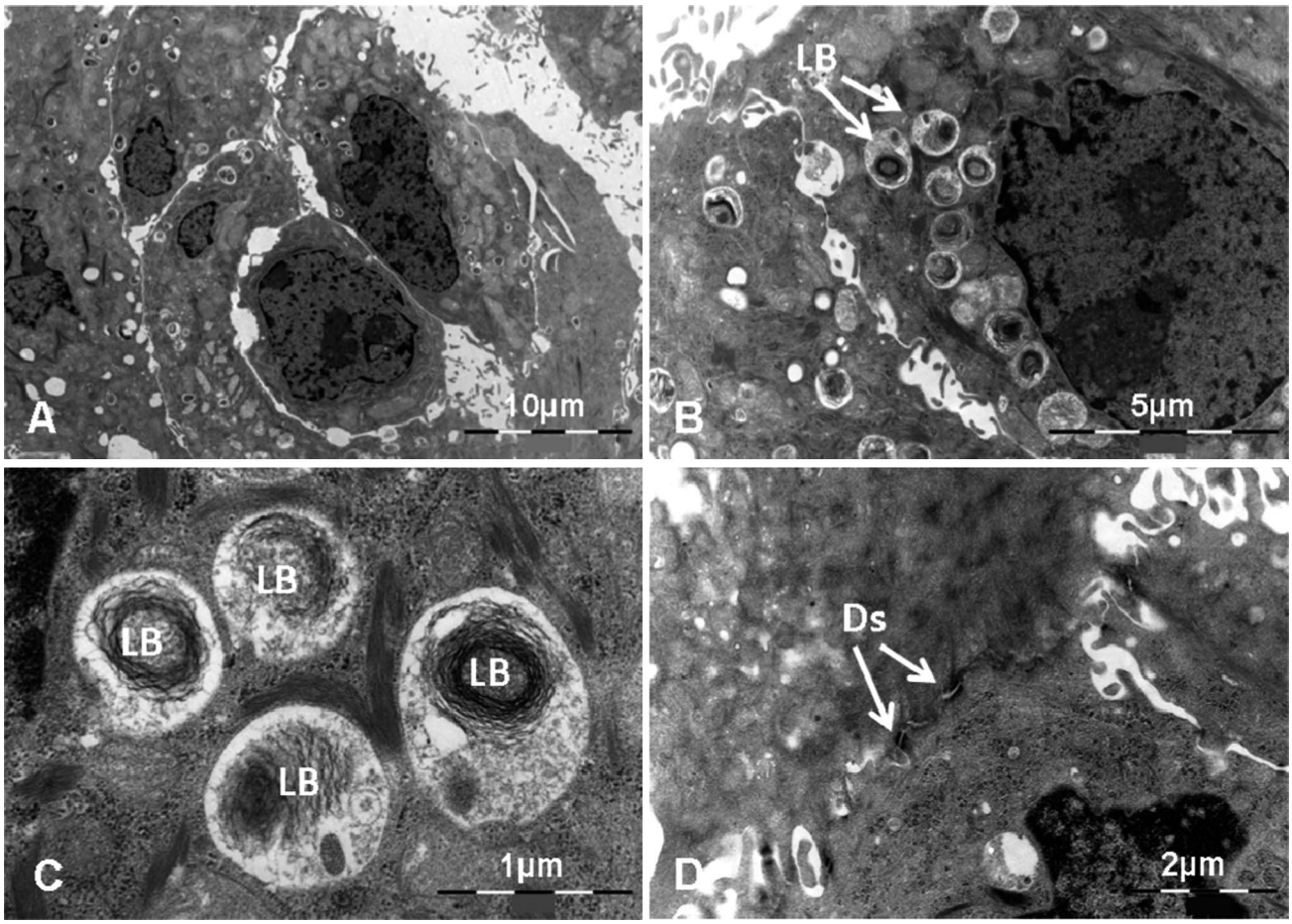

Fig. 5 TEM of A549 cells grown to confluence in the microfluidic channel before being wounded. (A and B) Horizontal sections showing tightly connected A549 cells and the formation of a confluent layer, (C) lamellar bodies (LB) that are exclusively present in type II alveolar epithelial cells and (D) desmosomes (Ds) can clearly be identified at higher magnification.

desmosomes can be identified confirming the presence of strong cell–cell contacts.

3.2. Epithelial wound creation

A focused flow of trypsin was used to generate a selective wound in the confluent A549 cell monolayer (Fig. 2). After 4 minutes of trypsin exposure at a 3.4 μl min^{-1} flow rate, morphological changes of the cells were observed in the middle of the channel. The cells became round and started to detach from the glass substrate. After two additional minutes of this treatment the cells located in the middle of the channel detached completely, leaving two intact, adjacent cell layers (Fig. 2b). The wound size was almost 300 μm after trypsinisation, which corresponds to 1/3 of the total width of the microchannel and indicates a stable establishment of the laminar flow during the wounding. Unlike standard scratch-tests routinely used for *in vitro* pulmonary epithelial wound-healing assays,[10,11,23] trypsin does not break cell membrane integrity of affected cells, but removes them gently without causing single cell injury. The loss of cellular membrane integrity consequently leads to cell death by necrosis and subsequent efflux of intracellular components into the surrounding milieu, potentially affecting the experimental outcome.

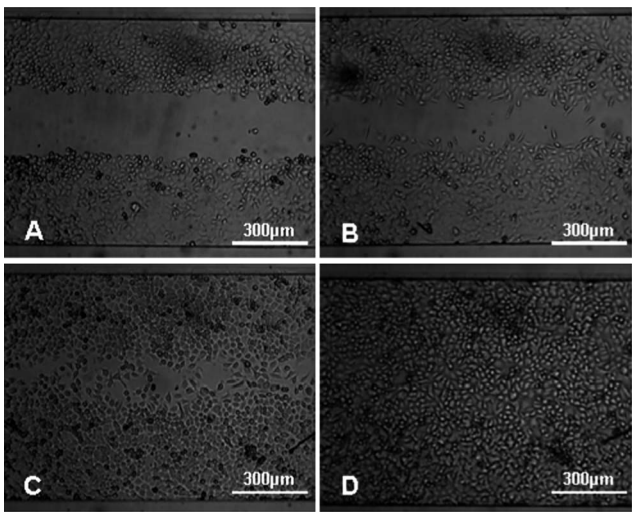

Fig. 6 Microscopic image sequence of the A549 cell monolayer showing the wound-healing process after trypsin wounding. The cells were perfused for 23 hours at 3.4 μl min^{-1} for one minute every 30 minutes with an enriched medium containing 10 ng ml^{-1} HGF. (A) Epithelial wound immediately after trypsin wounding and (B) after 5 h, (C) after 13 h (D) and after 23 h of HGF exposure.

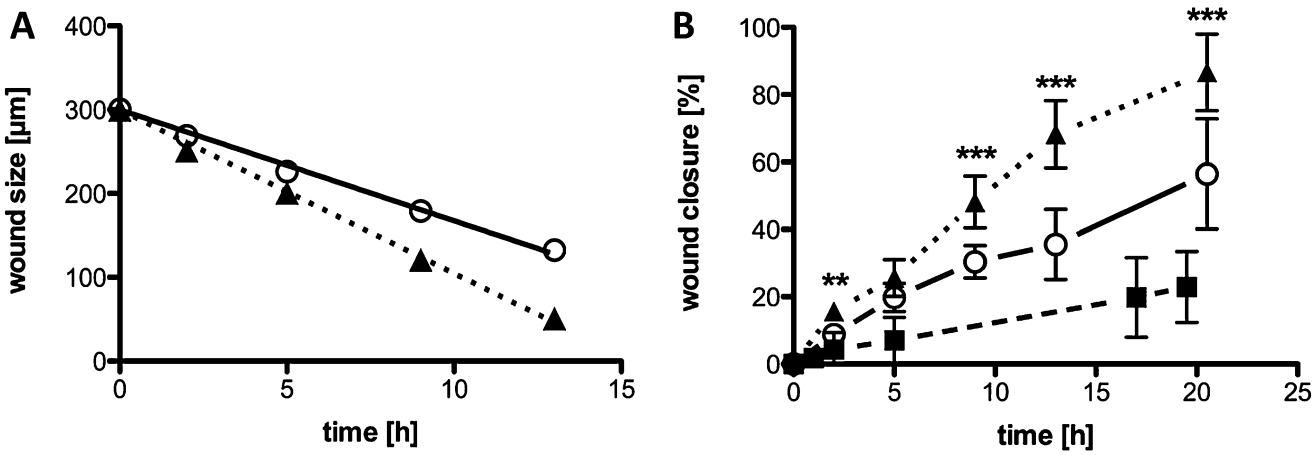

Fig. 7 (A) Representative example of wound size measurement over an experimental period of 13 hours. The regression analysis indicates the wound-healing rate, whereupon the more pronounced slope (▲ *vs.* ○) signifies a wound-healing benefit caused by HGF and (B) wound-healing of a wounded and differently treated epithelial cell (A549) monolayer. Filled squares (■) indicate culture conditions without the addition of any growth factor (serum-free). Open circles (○) represent the cell culturing in enriched media and filled triangles (▲) stand for the additional supplementation with 10 ng ml^{-1} HGF. Data are represented as mean values with 95% confidence intervals for $n = 4$, *p-value < 0.05, **p-value < 0.01, and ***p-value < 0.001.

3.3. Epithelial wound-healing

After wounding (Fig. 6a), the healing progression was monitored to investigate the effect of HGF on the regeneration of A549 cells. Three independent processes contribute to the wound closure. Immediately after injury, cells located at the wound edges flatten out and as a result spread out on the area denuded by trypsin. Then, cell migration takes place that can be observed at the cell morphological changes towards a polarized, spindle-shaped appearance. Finally, adequate wound-healing essentially depends on cellular proliferation.[24] Epithelial restitution consequently involves an initial spreading phase, followed by cellular migration and proliferation efforts all of which contribute to the closure of the wound. Its size continuously decreased over time and was completely closed after 23 h (Fig. 6d). We demonstrated that supplementation of enriched RPMI with 10 ng ml^{-1} HGF markedly increases the *in vitro* wound closure rate from 13.2 to 19.5 µm h^{-1} (Fig. 7a) corresponding to a 1.5 times increase in the wound closure rate. In accordance, these findings are very similar to the values obtained by van der Meer[15] with endothelial cells exposed to the vascular endothelial growth factor (VEGF) in a similar microfluidic system.

To assess whether this epithelial wound-healing benefit is due to enhanced cellular proliferation, increased migration or pronounced spreading, we examined the wound-healing in response to starved media (Fig. 7b; serum-free ○). The absence of serum causes the cells to enter the G0-phase and reduces their activity to the minimum. We observed that serum-deprivation has a substantial effect on epithelial regeneration in this wound-healing assay and prevents the remaining cells from adequate re-population of the denuded area. Indeed, even after more than 72 h of culture, the wound was not closed completely. Contrary

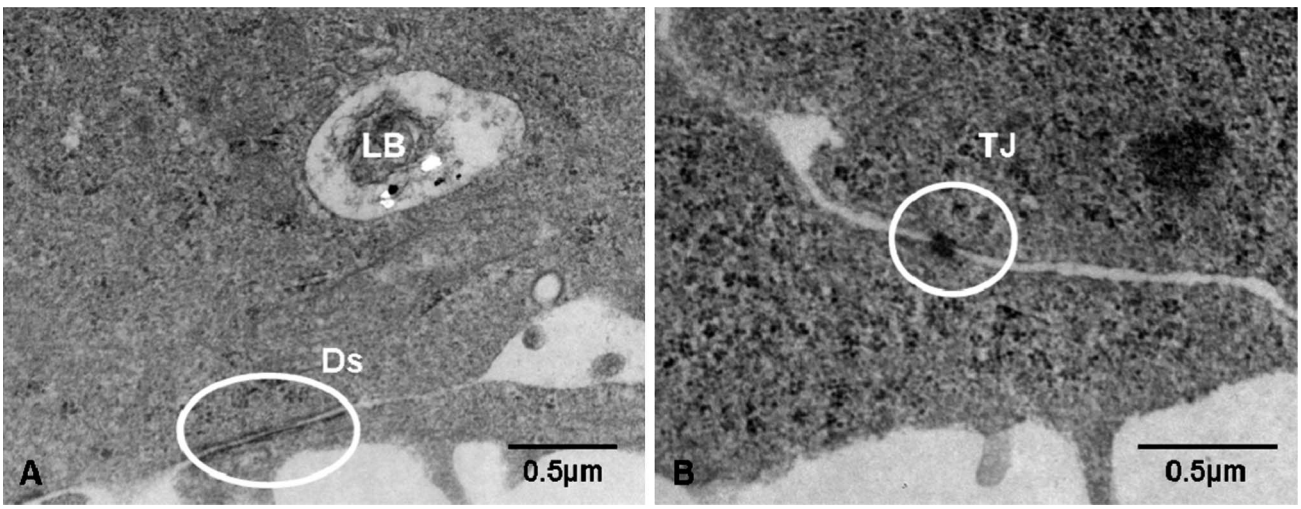

Fig. 8 TEM of vertical sections of A549 cell layer grown to confluence in the microfluidic channel, wounded with trypsin and regenerated under exposure to HGF-supplemented enriched media. (A) Electron-dense region at the cell–cell interface indicates a cell junction (CJ) protein accumulation and a lamellar body (LB) can be seen in this section, whereas (B) a tight junction (TJ) is apparent on this micrograph.

to the starved media, FBS supplementation was sufficient to induce complete wound-healing within the experimental observation period. Therefore, we conclude that cellular proliferation of the wound edging cells is essential for a proper wound-healing in this system and that the generated wound cannot be filled by cellular migration and spreading alone. To further support this assumption, we evaluated the effect of HGF on mitomycin C pre-treated A549 cells, a commonly available proliferation blocker. In fact, no difference between HGF supplementation and control treated cells was found (see ESI, Fig. S2†).

Further observations reveal that beside the continuous sheet movement of the wound borders, the morphology of some epithelial cells located at the edge of the wound changed from a cobblestone-like structure immediately after the wounding to a polarized, spindle-shaped and elongated one. These morphological changes indicate a migratory phenotype of these cells.

3.4. Characterization of the epithelial layer after healing

The morphology of the regenerated epithelial layer (Fig. 6d) is very similar to the one before injury. The epithelial layer exposed to HGF-supplemented enriched media was subjected to TEM investigation. Vertical TEM sections reveal the presence of apical tight junctions (Fig. 8b) as well as lamellar bodies (Fig. 8a), indicating that the phenotype of A549 cells is preserved along the whole experiment and that HGF exposure does not induce phenotypical changes. These data further indicate that the wounded epithelial monolayer is repaired by new type II alveolar epithelial-like cells derived from proliferated A549 cells. This further strengthens our hypothesis that HGF exerts its beneficial regenerative effect *via* induction of cellular proliferation.

4. Conclusions

In sharp contrast to standard scratch-tests routinely used for *in vitro* epithelial wound-healing assays, the presented microfluidic wound-healing system based on a focused flow of trypsin allows selective removal of cells without causing single-cell injuries. This system is used to investigate the regeneration of a wounded lung epithelial cell layer exposed to HGF. The effect of HGF on the healing rate is characterized and discriminated from the effect upon serum exposure. The presented results clearly show that in response to injury, alveolar epithelial cells spread, migrate and proliferate in a microfluidic environment. Based on assays performed with a proliferation blocker and HGF, we conclude that HGF treatment is predominantly due to enhanced cellular proliferation. It could also be shown that HGF treatment leads to accelerated and complete reestablishment of the epithelial barrier function with phenotypic preservation of type II alveolar epithelial cells before and after injury. Indeed, TEM investigations, a method that can also be used for cells cultured in microfluidic systems, particularly revealed that extensive cell–cell contacts and lamellar bodies, typical hallmarks of type II alveolar epithelial cells, were present in the regenerated cells. For this, EPON was introduced by capillary forces into the microchannel to embed the epithelial layer.

This microfluidic wound-healing system is an interesting alternative to conventional scratch tests, since the wounding can be better reproduced and the regeneration conditions can be regulated more precisely. Such a system could very well be used for personalised medicine approaches, where patient's material and cell numbers are usually very limited.

Acknowledgements

The authors wish to acknowledge the helpful discussions with Prof. Dr Barbara Rothen-Rüthishauser, from the Adolphe Merckle Institute of the University of Fribourg, Switzerland, and with Dr Fabian Blank, from the Department of Clinical Research of the University of Berne, Switzerland.

References

1 M. Selman, K. E. Talmadge and A. Pardo, *Ann. Intern. Med.*, 2001, **134**, 136–151.
2 R. M. Strieter and B. Mehrad, *Chest*, 2009, **136**, 1364–1370.
3 S. K. Frankel and M. I. Schwarz, *Curr. Opin. Pulm. Med.*, 2009, **15**(5), 463–469.
4 N. Walter, H. R. Collard and T. E. King, *Proc. Am. Thorac. Soc.*, 2006, **3**, 330–338.
5 M. Shiratori, G. Michalopoulos, H. Shinozuka, G. Singh, H. Ogasawara and S. L. Katyal, *Am. J. Respir. Cell Mol. Biol.*, 1995, **12**(2), 171–180.
6 R. A. M. Panganiban and R. M. Day, *Acta Pharmacol. Sin.*, 2011, **32**, 12–20.
7 L. Crosby and C. Waters, *Am. J. Physiol.: Lung Cell. Mol. Phys.*, 2010, **298**, L715–L731.
8 A. Gazdhar, P. Fachinger, C. van Leer, J. Pierog, M. Gugge, R. Friis, R. A. Schmid and T. Geiser, *Am. J. Physiol.: Lung Cell. Mol. Phys.*, 2006, **292**, L529–L536.
9 M. Poujade, E. Grasland-Mongrain, A. Hertzog, J. Jouanneau, P. Chavrier, B. Ladoux and A. Buguin, *Proc. Natl. Acad. Sci. U. S. A.*, 2007, **104**(41), 15988–15993.
10 S. Buckley, W. Shi, L. Barsky and D. Warburton, *Am. J. Physiol.: Lung Cell. Mol. Phys.*, 2008, **294**, L739–L748.
11 C. Neurohr, S. L. Nishimura and D. Sheppard, *Am. J. Respir. Cell Mol. Biol.*, 2006, **35**, 252–259.
12 G. Walker, H. Zeringue and D. Beebe, *Lab Chip*, 2004, **4**(2), 91–97.
13 G. M. Takayama, S. McDonald, J. C. Ostuni, E. Liang, M. N. Kenis, J. P. A. Ismagilov and R. F. Whitesides, *Proc. Natl. Acad. Sci. U. S. A.*, 1999, **96**, 5545–5548.
14 F. Nie, M. Yamada, J. Kobayashi, M. Yamato, A. Kikuchi and T. Okano, *Biomaterials*, 2007, **28**, 4017–4022.
15 A. D. Van der Meer, K. Vermeul, A. A. Poot, J. Feijen and I. Vermes, *Am. J. Physiol.: Heart Circ. Physiol.*, 2010, **298**, H719–H725.
16 J. C. McDonald and G. M. Whitesides, *Acc. Chem. Res.*, 2002, **35**, 491–499.
17 X. Zhu, L. Yi Chu, B. Chueh, M. Shen, B. Hazarika, N. Phadke and S. Takayama, *Analyst*, 2004, **129**(11), 1026–1031.
18 http://rsbweb.nih.gov/ij/index.html.
19 C. Neurohr, S. L. Nishimura and D. Sheppard, *Am. J. Respir. Cell Mol. Biol.*, 2006, **35**, 252–259.
20 F. Blank, B. Rothen-Rutishauser, S. Schurch and P. Gehr, *J. Aerosol Med.*, 2006, **19**(3), 392–405.
21 M. V. Kunnavakkam, *et al.*, *Appl. Phys. Lett.*, 2003, **82**(8), 1152.
22 A. J. Carterson, K. Höner zu Bentrup, C. M. Ott, M. S. Clarke, D. L. Pierson, C. R. Vanderburg, K. L. Buchanan, C. A. Nickerson and M. J. Schurr, *Infect. Immun.*, 2005, **73**(2), 1129–1140.
23 T. Geiser, P. H. Jarrea, K. Atabai and M. A. Matthay, *Am. J. Physiol.: Lung Cell. Mol. Phys.*, 2000, **279**(6), L1184–L1190.
24 J. M. Zahm, H. Kaplan, A. L. Hérard, F. Doriot, D. Pierrot, P. Somelette and E. Puchelle, *Cell Motil. Cytoskeleton*, 1997, **37**(1), 33–43.

